

Object Identification using Support Vector Regression for Haptic Object Reconstruction

Praveena W. Dewapura
Department of Electrical Engineering
University of Moratuwa
Moratuwa 10400, Sri Lanka
pwdewapura@gmail.com

K.D.Malith Jayawardhana
Department of Electrical Engineering
University of Moratuwa
Moratuwa 10400, Sri Lanka
malithjayawardhana@gmail.com

A. M. Harsha S. Abeykoon
Department of Electrical Engineering
University of Moratuwa
Moratuwa 10400, Sri Lanka
harsha@uom.lk

Abstract— The lack of realistic haptic feedback has become a significant barrier to achieve realization in virtual reality. If an object is to be reproduced in the haptic dimension, it's essential to analyze the object behavior for mechanical inputs. Nevertheless, prior studies have considered model-based approaches to model the behavior of the real object for reconstruction, and the conventional spring-damper model was the most widely used. However, proper object identification is crucial in accurate haptic object modeling for reconstruction. Thus, this paper proposes an AI-based approach using a nonlinear regression algorithm, Support Vector Regression (SVR). AI algorithm predicts the object's response for motion parameters by analyzing the nonlinear responses from the object extracted through a sensorless sensing system based on Disturbance Observer (DOB) and Reaction Force Observer (RFOB). Furthermore, the viability of the proposed approach is demonstrated by comparing it to the conventional model-based approach.

Keywords— haptic information, virtual reality, Disturbance Observer, force response, virtual object reconstruction, Artificial Intelligence, Support Vector Regression.

I. INTRODUCTION

In the ever-evolving world of technology, realistic haptic feedback takes ceaseless importance to achieve realization in virtual reality [1]. Nevertheless, most studies are still lagging in creating the pure experience of touch feedback, and thus, they fail to develop the objects' actual perception in the haptic dimension.

Haptic information is bilateral and involves action and reaction. The reaction from an object includes not only motion and force information but also its impedance. Thus, the real contribution of all these factors should be evaluated and understood from the real environment for precise object identification for reconstruction.

Numerous studies have employed model-based approaches in defining the behavior of the object on contact and utilized those to simulate haptic sensation [2]-[4]. Many studies have acknowledged the conventional spring-damper model to model the real object [2]-[4]. Consequently, the behavior of the object impedance was predefined with the aid of stiffness and viscosity whose functionalities were assumed as constant or exponential or polynomial [2] which contradict the real behavior of the object impedance [5]. Researchers have also utilized the mass-spring-damper model by integrating mass with the spring-damper model to define the object behavior. Hence, the object behavior was primarily identified as a spring-damper while ignoring its nonlinear behavior of responses [5]. Despite its invalidity [5], the spring-damper behavior was considered to interpret interaction with the virtual object and thereby deduced the interaction forces

that occur when touching the virtual object in the haptic rendering algorithm [4].

Moreover, the impact of learnt force on reproduction needs much attention and still, haptic studies merely consider only motion data. Force information was used with the motion information to improve the quality of the grasp performed by the strain gauge-based cyber glove [4]. However, the force magnitudes were measured using force sensors regardless of their drawbacks such as signal noise, narrow bandwidth, complicity, non-collocation, and instability [6], [7]. To overcome these problems, Kouhei Ohnishi *et al.* have introduced a sensorless force control with a broad bandwidth realized using Disturbance Observer (DOB) [8], [9] and Reaction Force Observer (RFOB) [6], [10]. The motion-copying system (MCS) has been developed based on DOB and RFOB to reproduce force and position information saved in motion-data memory by bilateral teleoperation [11]. However, the MCS simply playback haptic information using motion saving and loading functionalities and it has ignored the reconstruction phase of the virtual object. Thus, this system was only capable of reproducing saved position and force information while losing generalization.

However, recent studies have integrated machine learning and deep learning techniques to achieve faster and accurate results. A Convolutional Neural Network (CNN) has been used to estimate path by combining depth information and grasping motion towards the object in a motion reproduction system [12]. Hence, these researchers have reproduced grasping force through kinematics equations by analyzing motion data abstracted using depth sensors. Thus, they have considered vision information to identify the object and analyze motion data ignoring the real potential of sense of touch. A neural network has been used to estimate external forces from motion parameters in a model-independent neural network force observer [13]. Despite the drawbacks, force sensors were used in the training phase of the neural network to measure contact forces [6], [7]. A nonlinear regression model, Support Vector Regression (SVR) has been used to infer the haptic force positions in unseen stimulation locations on the 3D structure to achieve haptic sensation through learning deformation patterns [14]. However, the force measurements of this study have also relied on strain gauges despite their issues [6], [7].

Hence, it is evident that identifying the real object behavior is critical for object reconstruction in the haptic dimension. Therefore, this paper proposes an object identification approach based on AI for haptic object reconstruction. Thus, the AI-based approach using the SVR algorithm is presented to predict the force response by learning haptic information extracted through the DOB and RFOB based sensorless sensing system.

II. METHODOLOGY

The reconstruction of the virtual haptic object depends on how well the object is identified by incorporating its actual nonlinear behavior and consequently how well the object is modeled to mimic the actual behavior of the object. Hence, two object identification approaches can be recognized for reconstruction along with the proposed approach.

- Model-based approach.
- AI-based approach.

Since the AI-based approach relies on data, it is essential to collect enough data to develop the AI model. Thus, the research procedure followed two phases as illustrated in Fig. 1.

- Abstraction phase.
- Reconstruction phase.

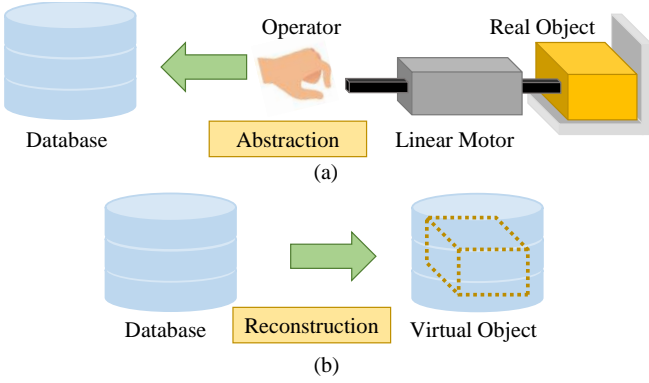


Fig. 1. Representation of a) Abstraction phase and b) Reconstruction phase of the haptic object.

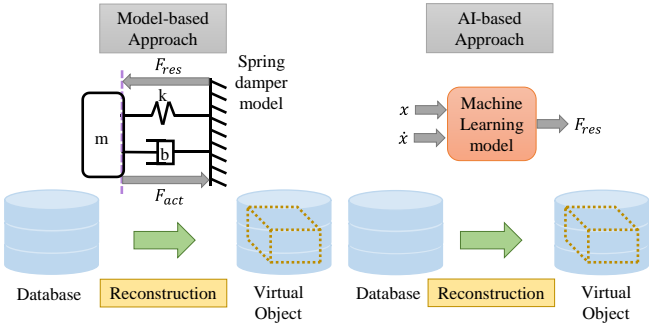


Fig. 2. Object identification approaches for reconstruction: Model-based approach and AI-based approach.

The system abstracts motion and force information for a specific force command applied to the object during the abstraction phase. Haptic information was gathered relevant to one object throughout this phase, and that object used on contact by the end effector of the linear motor was a sponge. During the reconstruction phase, a virtual object was developed using abstracted haptic information. Two separate virtual sponge objects were reconstructed to replicate the actual object behavior corresponding to each of these approaches. Fig. 2 compares the proposed AI-based approach to the conventional model-based approach.

All parameters used in this paper are shown in Table I.

A. Abstraction phase

The abstraction phase involves the acquisition of motion information with the corresponding responses from the object. Force sensors have been used in conventional force control to detect force despite their issues. However, force sensors can only detect external forces at their installed position, and the sensor itself adds mass or inertia to the system. Therefore, a DOB and RFOB based sensorless approach was employed to detect vivid force sensation with broad bandwidth. DOB was used to achieve robust force control, and RFOB was used to measure reaction force from the object.

TABLE I. NOMENCLATURE

Symbol	Description
M	Motor mass
M_n	The nominal value of motor mass
K_f	Motor force constant
K_{fn}	The nominal value of force constant
I_a^{ref}	Motor current
B	Viscosity coefficient
g_{dis}	Cut off frequency of DOB
g_{rec}	Cut off frequency of RFOB
x	Compression depth
\dot{x}	Velocity
F_m	Generated motor force
F_{dis}	Disturbance force
F_{ext}	Reaction force
F_{int}	Interactive force
F_f	Static friction
F_{cmd}	Force command
F_{res}	Force response
F_{act}	Action force
K_p	Proportional gain of PID controller
g_v	Velocity filter constant
\hat{F}_{dis}	Estimated disturbance force
\hat{F}_{ext}	Estimated reaction force
F_{res}^{cal}	Calculated force response
F_{res}^{pred}	Predicted force response

The disturbance observer observes the disturbance force of the system without using force sensors [8], [9]. This force can be derived as in (1) and (2) using equations from (3) – (7).

$$F_{dis} = F_{ext} + F_{int} + (F_f + B\dot{x}) + (M - M_n)\ddot{x} + (K_{fn} - K_f)I_a^{ref} \quad (1)$$

$$F_{dis} = K_{fn}I_a^{ref} - M_n\ddot{x} \quad (2)$$

The generated motor force, F_m can be express as shown in (3).

$$F_m = K_f I_a^{ref} \quad (3)$$

By applying the dynamic equation to the linear motor:

$$F_m - F_l = M\ddot{x} \quad (4)$$

Load force, F_l can be expressed as in (5).

$$F_l = F_{int} + F_{ext} + (F_f + B\dot{x}) \quad (5)$$

Since parameters, K_f and M are subjected to variations and estimation errors, they can be re-written in terms of nominal values and variations.

$$M = M_n + \Delta M \quad (6)$$

$$K_f = K_{fn} + \Delta K_f \quad (7)$$

Then, the estimated disturbance force is derived by passing disturbance through the low pass filter and suppressing noise due to the differentiator as in (8).

$$\hat{F}_{dis} = \frac{g_{dis}}{(s+g_{dis})} F_{dis} \quad (8)$$

The DOB is modified as RFOB to estimate the reaction force by identifying the internal disturbance in the system without using a force sensor [6],[10]. Thus, RFOB acts as a virtual force sensor in estimating only the reaction force. The estimated reaction force can be represented as in (9) and (10).

$$\begin{aligned} \hat{F}_{ext} = & \frac{g_{rec}}{(s+g_{rec})} (K_{fn} I_a^{ref} + M_n g_{rec} \dot{x} - \\ & (F_{int} + F_f + B\dot{x} + (M - M_n)\ddot{x} + \\ & (K_{fn} - K_f) I_a^{ref}) - M_n g_{rec} \dot{x} \end{aligned} \quad (9)$$

$$\hat{F}_{ext} = \frac{g_{rec}}{(s+g_{rec})} F_{ext} \quad (10)$$

The block diagrams of the function of disturbance force observation by the DOB and the function of reaction force estimation by the RFOB are shown in Fig. 3. Fig. 4 shows the overall block diagram of the abstraction phase with the force control mechanism using DOB and RFOB.

B. Reconstruction phase

The reconstruction phase involves developing the respective virtual object model by identifying object behavior through each approach using motion information. Hence, compression depth and filtered velocity were considered to analyze the object's response through both approaches.

A labeled dataset of 5,200,000 samples was extracted for a ramped force command applied on the sponge object. However, a reduced version of the dataset was used in this analysis. Fig. 5 depicts the variation of recorded haptic information relative to time and motion parameters. The obtained structured dataset was divided into two subsets for training and testing as mentioned in Table II. The training set was used to build the virtual object model by identifying the relationship between force information and motion parameters. The testing set was used to test the virtual representation by comparing the actual values with the estimated values. Moreover, these two datasets are separate

datasets that aren't composed of any data common to both datasets. Hence, during the training process, the test set samples were not considered.

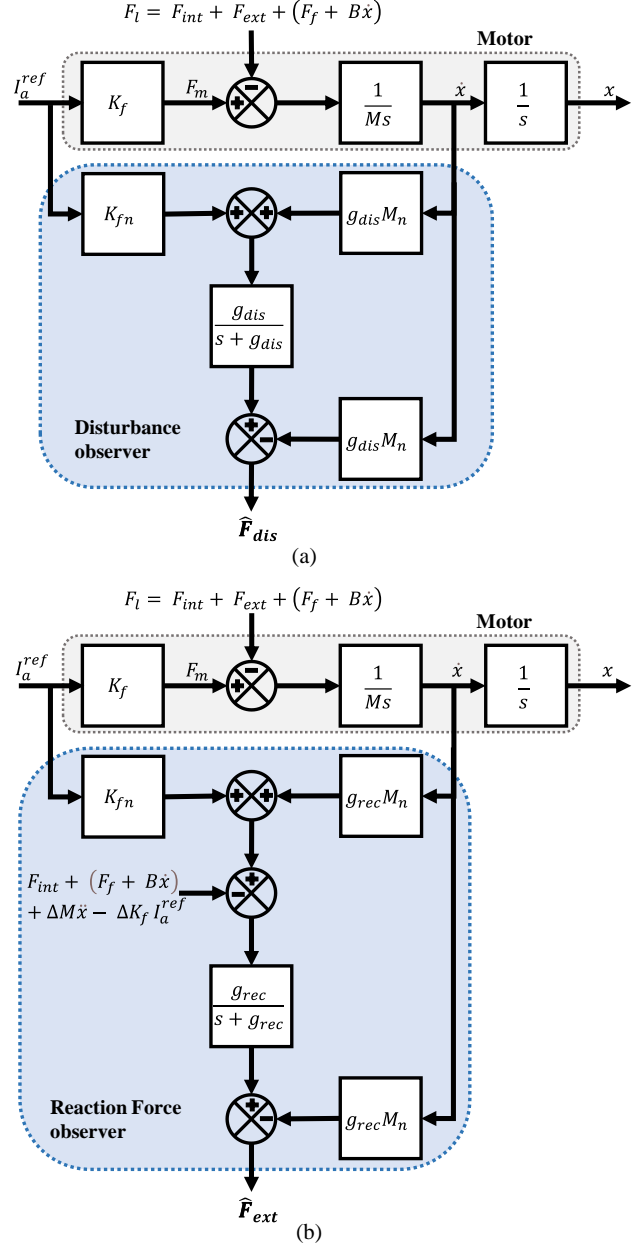


Fig. 3. Block diagrams (a) Disturbance Observer (b) Reaction Force Observer.

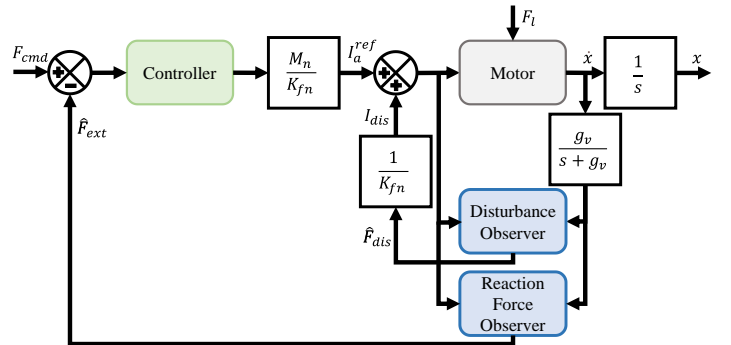


Fig. 4. Force controller based on DOB and RFOB.

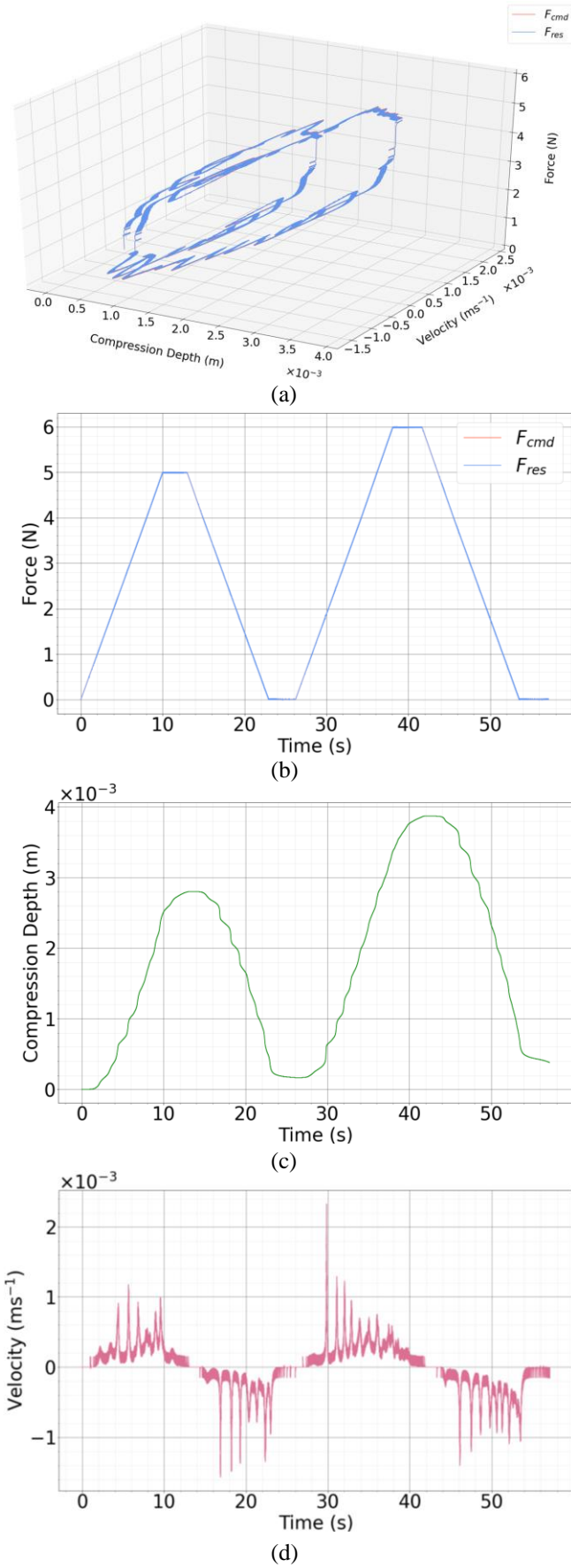


Fig. 5. a) Force profile on the object over motion parameters b) Force profile on the object over time c) Compression depth profile on the object over time d) Velocity profile on the object over time.

TABLE II. TRAIN - TEST DATASETS

Dataset	No. of samples
Training dataset	24000
Testing dataset	28000

The performance of the object identification approaches was evaluated using regression metrics and thereby, decided the best approach in object identification for reconstruction. Thus, regression metrics considered for model performance evaluation used in this study are,

- R^2 score
- Mean absolute error (MAE)
- Mean squared error (MSE)
- Root mean squared error (RMSE)

1) *Model-based approach*: The most commonly used spring-damper combination was considered in this analysis. Therefore, force response was defined by considering the combinational effect of the forces from the spring, and the damping force. Equation (11) denotes the relationship between the force response and the motion parameters.

$$F_{res} = F_k + F_b = kx + b\dot{x} \quad (11)$$

The environment impedance has been considered as a function of its motion parameters in spring damper modeling. Hence, the values of stiffness coefficient, k , and the damping coefficient, b were obtained assuming their behavior as constant for the training data set using the curve fitting tool in Matlab. Then, these values were used to calculate force responses, F_{res}^{cal} for the test set samples.

2) *AI-based approach*: The force response from the object was derived considering compression depth and velocity parameters in the conventional spring-damper modeling. Thus, the extracted features for the AI model to predict the force response are,

- Compression depth (x)
- Velocity (\dot{x})

Fig. 6 manifests the proposed AI-based approach using the SVR algorithm.



Fig. 6. SVR Model

The range of all features was normalized using min-max scaling to achieve higher accuracy. Equation (12) is the normalization formula used.

$$y' = \frac{y - y_{min}}{y_{max} - y_{min}} \quad (12)$$

where y' represents the normalized value of the feature y . y_{min} and y_{max} are the minimum and the maximum values of the feature. This normalization procedure was carried out separately on the training and testing datasets.

The proposed AI-based approach is based on multi-label regression that uses supervised learning. Hence, a nonlinear regression model, Support Vector Regression (SVR) [15], [16] was used to build the virtual sponge object. The SVR algorithm is a powerful kernel-based learning algorithm and a very effective method for learning complex nonlinear functions. For the given training data $\{(a_1, b_1), \dots, (a_n, b_n)\} \subset \mathcal{A} \times \mathbb{R}$ and where $\mathcal{A} \in \mathbb{R}^2$ denotes the space of the input features, the SVM model can be defined as is (13).

$$f(a, w) = \langle a, w \rangle + d \quad (13)$$

where vector $w \in \mathcal{A}$, scalar $d \in \mathbb{R}$ and $\langle \cdot, \cdot \rangle$ denotes the dot product in \mathcal{A} . The SVR algorithm has a convex optimization and the minimization function of the SVR algorithm can be represented as in (14).

$$L = \text{MIN} \frac{1}{2} \|w\|^2 + C \sum_{i=1}^n (\xi_i + \xi_i^*) \quad (14)$$

subjected to,

$$b_i - \langle a_i, w \rangle - d \leq \varepsilon + \xi_i$$

$$\langle a_i, w \rangle + d - b_i \leq \varepsilon + \xi_i^*$$

where ε is the precision, $\xi_i, \xi_i^* \geq 0$ are slack variables and $C > 0$ is a constant which determines the trade-off between the regression model's complexity. The SVR algorithm uses kernel functions to transform the feature vectors to another space to overcome nonlinearity. The popular kernel function, radial basis function (RBF) was used in this study as shown in (15).

$$K(a_i, a_j) = \exp(-\gamma \|a_i - a_j\|^2) \quad (15)$$

where $\gamma > 0$ is the kernel coefficient for RBF. The hyperparameters of the SVR model were tuned to define the SVR model that is performing well on the training dataset. Then, the defined model was used to train the SVR model for the sponge object identification using the training dataset. Finally, the trained SVR model was used to predict the force responses, F_{res}^{pred} for the testing dataset. The python sklearn [17] implementation of the SVR algorithm was used in this study.

III. EXPERIMENTAL SETUP



Fig. 7. Experimental setup for the abstraction of haptic information.

The experimental setup used in the acquisition of haptics information is shown in Fig. 7. The research focused on object identification for reconstruction by replicating 1 DOF haptics interaction. Thus, a linear motor was implemented as the actuator and a linear encoder was used to obtain compression depth. A sponge was considered as the object in identification for reconstruction in this experiment. The control software for

this system was programmed using C language on mbed microcontroller analog/digital I/O | Model 826. The values of experimental parameters are listed in Table III. In this study, the initial position of the actuator was set on the surface of the object and obtained relevant motion information.

TABLE III. EXPERIMENTAL PARAMETERS

Symbol	Value
M_n	0.46 kg
K_{fn}	24 N/A
g_{dis}	300 rad/s
g_{rec}	300 rad/s
K_p	2
g_v	30

IV. RESULTS AND DISCUSSION

The spring-damper model was the model-based approach considered in this analysis. Thus, the best matching values for stiffness and viscosity were generated through the curve fitting tool in Matlab by assuming their behavior as constant. Consequently, the relationship between the force response and motion parameters was deduced as exhibited in (16). The profile of force response was simulated using the curve fitting tool from the training dataset as shown in Fig. 8 and the surface of the generated function can be identified in the same figure.

$$F_{res} = 1624x + 2331\dot{x} \quad (16)$$

The calculated force responses for the test set samples were obtained using the relationship shown in (16). Therefore, all calculated force responses of the test dataset will lie on the same plane which is generated by the function. The graphs in Fig. 9 show how the calculated force responses, F_{res}^{cal} using the spring-damper model vary from the actual force responses.

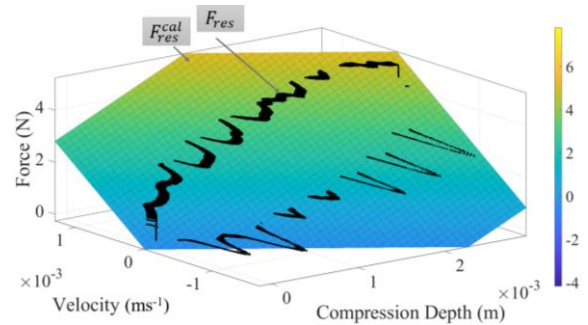


Fig. 8. Simulated force response from the spring-damper model.

In the AI-based approach, the SVR algorithm was chosen to build the virtual object model. Since the SVR method is convexing, it guarantees to produce a global solution. However, the relationship between motion parameters and force response cannot be simply defined as the spring damper modeling in the AI-based approach. Hence, the kernel function was used to transform the nonlinear input feature space into another space to identify the nonlinear behavior. The hyperparameters of the algorithm were tuned to adjust the algorithm along with its kernel function to have higher performance on the training set. Table IV lists the specific hyperparameter values which were chosen to define the SVR model to achieve better performance on the training dataset.

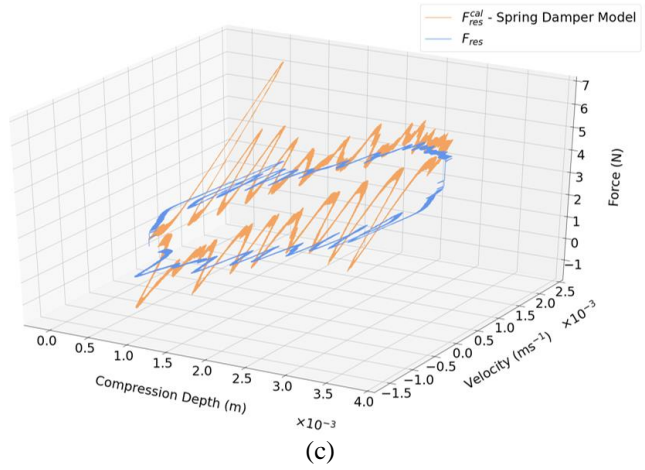
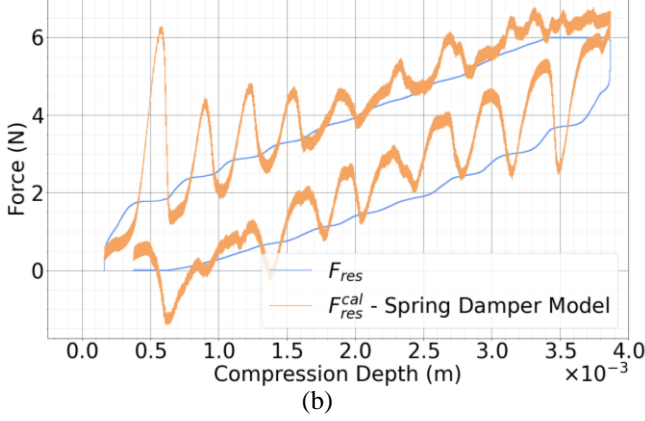
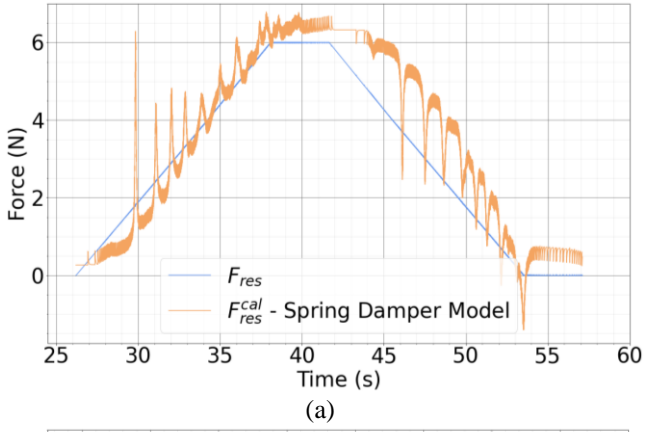


Fig. 9. Spring-damper model results for a sponge object a) Calculated force response over time b) Calculated force response over compression depth c) Calculated force response over motion parameters.

The trained SVR model was used to generate predictions for the test set samples in the AI-based approach. The graphs in Fig. 10 explain how the predicted force responses, F_{res}^{pred} using the SVR model deviate from the actual force responses.

TABLE IV. HYPERPARAMETERS OF SVR MODEL

Hyperparameter	Value
Kernel Type	'rbf'
Kernel coefficient for 'rbf' (γ)	0.002
Regularization parameter (C)	0.1
Precision (ϵ)	0.0001

$$Accuracy = 1 - RMSE \quad (17)$$

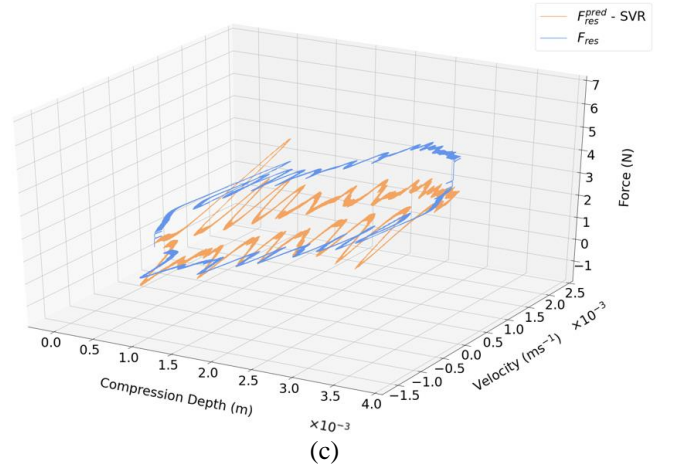
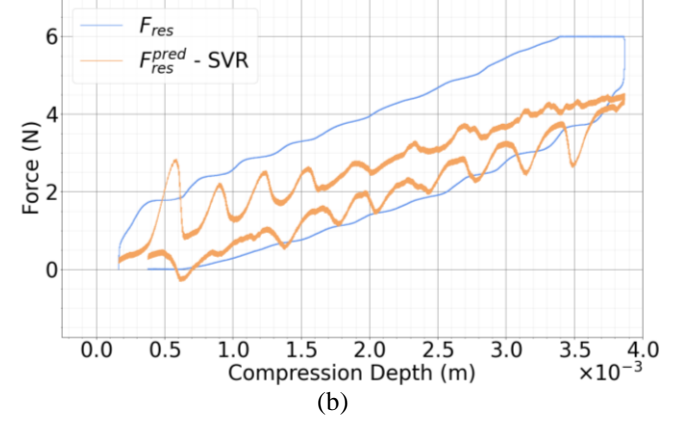
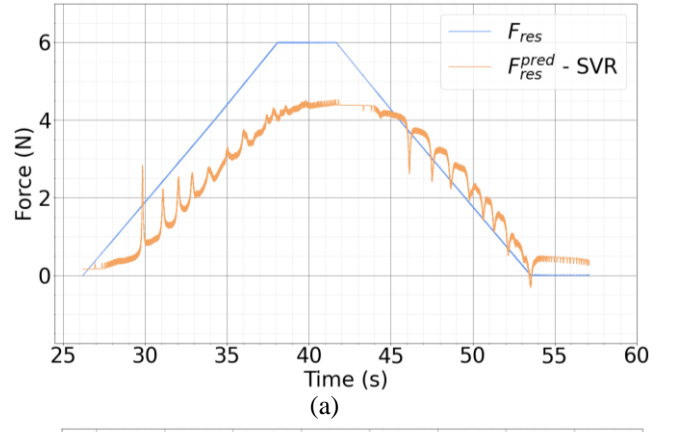


Fig. 10. SVR algorithm results for a sponge object a) Predicted force response over time b) Predicted force response over compression depth c) Predicted force response over motion parameters.

The performance of both models was evaluated using regression matrices. Table V outlines the comparison of these regression matrices for the two approaches considered and Fig. 11 summarizes the same. The virtual model should have a higher R^2 score and lower regression losses denoted by MAE, MSE, and RMSE for the model to perform well. When comparing R^2 score values of both approaches, it seems that the traditional model-based approach performed better than the AI-based approach. However, the R^2 score is not a more reliable metric to be considered in the nonlinear analysis because the R^2 score reflects the correlation that indicates linearity. Hence, RMSE was considered in this analysis and it was discovered that the AI algorithm was performing better than the spring-damper model in replicating the object's behavior. Furthermore, as shown in Fig. 12 the SVR algorithm

is capable of identifying the object up to an accuracy of 82.7% in sense of RMSE as derived in (17). Thus, the AI-based approach is better than the model-based approach in evaluating the nonlinear behavior of responses of the object which cannot be interpreted using simple mathematical representation. Therefore, it is visible that AI-based virtual object modeling is the best approach to identifying the object for reconstruction.

TABLE V. COMPRESSION OF REGRESSION METRICS

Regression Metric	Spring Damper model	SVR algorithm
R^2 score	0.81	0.75
MAE	0.71	0.15
MSE	0.81	0.03
RMSE	0.90	0.17

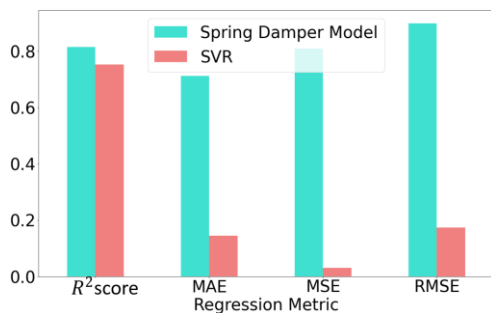


Fig. 11. Comparison of Regression Metrics for virtual object models.

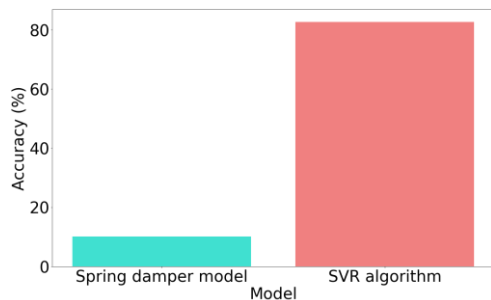


Fig. 12. Comparison of Accuracy for virtual object models.

V. CONCLUSION

This paper proposed an AI-based approach for replicating the real behavior of the sponge object while incorporating its nonlinear behavior of responses. In the AI-based approach, a simple mathematical interpretation cannot be defined as in the spring-damper model-based approach. Hence, the AI-based approach would be preferable in identifying the object's nonlinear behavior, which cannot be defined using a simple mathematical representation. Thus, a nonlinear regression algorithm, SVR was chosen to develop the AI model for the object. The SVR algorithm uses kernel functions to transform the nonlinear feature vectors to another space and the 'rbf' kernel was used in this study. Therefore, the SVR algorithm predicted the force response using motion parameters that are compression depth, and velocity by incorporating the nonlinear behavior of the object.

The proposed AI-based approach was compared with the most commonly used spring-damper model-based approach. Hence, regression metrics of both virtual object models were evaluated, and discovered that the AI-based approach performed better than the model-based approach in virtual

object reconstruction. Moreover, the proposed AI-based approach identified the object with an accuracy of 82.7% in sense of RMSE. Thus, it clarifies that the AI-based approach outperforms the traditional model-based approach in identifying object behavior. Therefore, more promising results can be achieved when reproducing realistic haptic feedback using reconstructed haptic objects identified through AI-based approaches than model-based approaches.

ACKNOWLEDGMENT

The authors gratefully acknowledge the support provided by the Senate Research Committee, University of Moratuwa (SRC/LT/2020/21).

REFERENCES

- [1] H. Culbertson, S. B. Schorr, and A. M. Okamura, "Haptics: The present and future of artificial touch sensation," *Annual Review of Control, Robotics, and Autonomous Systems*, vol. 1, pp. 385–409, 2018.
- [2] T. Shimono, S. Katsura, and K. Ohnishi, "Abstraction and reproduction of force sensation from real environment by bilateral control," *IEEE Transactions on Industrial Electronics*, vol. 54, no. 2, pp. 907–918, 2007.
- [3] A. H. S. Abeykoon and K. Ohnishi, "Bilateral control interacting with a virtual model and environment," in *2006 IEEE International Conference on Industrial Technology*. IEEE, 2006, pp. 1320–1325.
- [4] A. M. Schmidts, D. Lee, and A. Peer, "Imitation learning of human grasping skills from motion and force data," in *2011 IEEE/RSJ International Conference on Intelligent Robots and Systems*. IEEE, 2011, pp. 1002–1007.
- [5] R. Ruwanthika and A. H. S. Abeykoon, "3d environmental force: Position impedance variation for different motion parameters," in *2015 Moratuwa Engineering Research Conference (MERCon)*. IEEE, 2015, pp. 112–117.
- [6] S. Katsura, Y. Matsumoto, and K. Ohnishi, "Modeling of force sensing and validation of disturbance observer for force control," *IEEE Transactions on industrial electronics*, vol. 54, no. 1, pp. 530–538, 2007.
- [7] I. S. Khalil and A. Sabanovic, "Sensorless torque/force control," *Advances in Motor Torque Control*, pp. 49–69, 2011.
- [8] K. Ohnishi, M. Shibata, and T. Murakami, "Motion control for advanced mechatronics," *IEEE/ASME transactions on mechatronics*, vol. 1, no. 1, pp. 56–67, 1996.
- [9] T. Shimono, S. Katsura, and K. Ohnishi, "Improvement of operability for bilateral control based on nominal mass design in disturbance observer," in *31st Annual Conference of IEEE Industrial Electronics Society*, 2005. IECON 2005. IEEE, 2005, pp. 6–pp..
- [10] T. Murakami, F. Yu, and K. Ohnishi, "Torque sensorless control in multidegree-of-freedom manipulator," *IEEE Transactions on Industrial Electronics*, vol. 40, no. 2, pp. 259–265, 1993.
- [11] S. Katsura, W. Yamanouchi, and Y. Yokokura, "Real-world haptics: Reproduction of human motion," *IEEE Industrial Electronics Magazine*, vol. 6, no. 1, pp. 25–31, 2012.
- [12] X. Sun, T. Nozaki, T. Murakami, and K. Ohnishi, "Grasping point estimation based on stored motion and depth data in motion reproduction system," in *2019 IEEE International Conference on Mechatronics (ICM)*, vol. 1. IEEE, 2019, pp. 471–476.
- [13] A. C. Smith, F. Mobasser, and K. Hashtrudi-Zaad, "Neural-network-based contact force observers for haptic applications," *IEEE Transactions on Robotics*, vol. 22, no. 6, pp. 1163–1175, 2006.
- [14] H. Sun and G. Martius, "Robust affordable 3d haptic sensation via learning deformation patterns," in *2018 IEEE-RAS 18th International Conference on Humanoid Robots (Humanoids)*. IEEE, 2018, pp. 846–853.
- [15] C. Cortes and V. Vapnik, "Support-vector networks," *Machine learning*, vol. 20, no. 3, pp. 273–297, 1995.
- [16] A. J. Smola and B. Schölkopf, "A tutorial on support vector regression," *Statistics and computing*, vol. 14, no. 3, pp. 199–222, 2004.
- [17] F. Pedregosa, G. Varoquaux, A. Gramfort, V. Michel, B. Thirion, O. Grisel, M. Blondel, P. Prettenhofer, R. Weiss, V. Dubourget et al., "Scikit-learn: Machine learning in python," *The Journal of machine Learning research*, vol. 12, pp. 2825–2830, 2011.